Investigation of Aerodynamic Profile Losses for a Low-Reaction Steam Turbine Blade

Hunter B. Guilliams

Thesis submitted to the faculty of the Virginia Polytechnic Institute and State University in partial fulfillment of the requirements for the degree of

Master of Science
In
Mechanical Engineering

Wing F. Ng, Co-Chair
Srinath Ekkad, Co-Chair
K. Todd Lowe

December 10, 2013
Blacksburg, VA

Keywords: steam turbine, low-reaction blades, profile loss

Investigation of Aerodynamic Profile Losses for a Low-Reaction Steam Turbine Blade

Hunter B. Guilliams

ABSTRACT

This thesis presents the results of a linear cascade experiment performed on the mean-line and near-tip sections of a low-reaction steam turbine blade and compares them to CFD of the former. The purpose of these tests was the refinement of a proprietary empirical profile loss model. A review of the literature shows that experimental data on this type of blade is not openly available. The continued efficacy of empirical loss models to low-reaction steam turbine blades requires data from experiments such as the present study. Tests covered a range of incidence from -6° to +4° and exit Mach numbers from 0.4 to 0.6. Extensive static pressure taps on the blades allowed detailed examinations of blade loading. This loading was dissimilar to steam turbine blade loading in the open literature. A traversing five-hole probe measured conditions downstream of the blade row to enable the calculation of a total pressure loss coefficient. The area-averaged total pressure loss coefficient for both profiles was near 0.08 and was not sensitive to incidence or exit Mach number over the ranges tested.

To Rachel. Without her, all is vanity.

Acknowledgements

Firstly, I express my gratitude to the Elliott Group for sponsoring this project. This work depended entirely on the efforts of Diganta Narzary, Nikhil Rao, and David Stasenko.

Next, I would like to thank Dr. Todd Lowe for leading me down the first tentative steps into the exciting field of turbomachinery and propulsion.

I would also like to express my appreciation to Dr. Srinath Ekkad. He has been an insightful technical leader throughout this project, but more importantly, he has helped me navigate the even more complex world of academia.

Dr. Wing Ng has been a constant motivator and mentor to me over the last year and a half. He has seen me through the incredibly difficult challenges associated with this program, and for those reasons and many more I owe him immeasurable thanks.

A group of people who can scarcely receive enough credit for this work are the staff of the Mechanical Engineering Department. My navigation to a degree simply would not have happened without the help of Mrs. Cathy Hill and Mrs. Marie Trimmer. Mrs. Diana Israel, when confronted with my dangerously late purchase orders offered companionship instead of chastisement. Johnny, Bill, James, Timmy, and Phillip of the ME machine shop have literally made the project and have helped me to hone my design skills.

The involvement of my fellow students in this project has been an enormous and invaluable help. I am thankful to Dorian Blot and Arnab Roy for working tirelessly to teach me their experimental methods. Ryan Nunes began the project before I arrived and was my colleague through most of its duration. His CFD is just one of his many significant contributions to this effort. Sakshi Jain has been a great help in processing the enormous amount of data generated and has contributed a constant stream of calm proficiency to this undertaking. Fellow graduate students who have assisted in the experiments include James Phillips, Kevin Peterson, Sean Brennan, and Allan Arisi. I have also had the pleasure of working with many excellent undergraduate researchers including David Mayo, Raul Otero, and Avi Friedman.

The efforts of all the aforementioned persons would not have gotten me through this project without the constant, loving support of my friends and family. Most affected by all of my long hours and late nights has been my wife Rachel. I'm not sure she knew exactly what she was signing up for when she married me in the middle of this work, but it is her presence in my life that has given me the endurance to see it through to the end.

Table of Contents

1. Introduction 1
   1.1 Steam turbine use 1
   1.2 Loss mechanisms 2
   1.3 Blade reaction 2
2. Literature review 4
   2.1 Loss models 4
   2.2 Application of loss models to modern blades 4
   2.3 Recent experiments on steam turbine airfoils 5
3. Experimental setup 6
   3.1 Virginia Tech Transonic Tunnel 6
   3.2 Upstream and downstream instrumentation 9
   3.3 Blade profiles 10
   3.4 Blade loading instrumentation 11
4. Results and discussion 12
   4.1 Blade loading 12
      4.1.1 Blade loading equations 12
      4.1.2 Comparison of experimental blade loading 12
      4.1.3 Comparison of blade loading with open literature 13
      4.1.4 Comparison of blade loading with CFD results 15
      4.1.5 Effect of incidence angle on blade loading 16
      4.1.6 Effect of exit Mach number on blade loading 16
   4.2 Traverse measurements 17
      4.2.1 Upstream traverse measurements 17
      4.2.2 Downstream traverse measurements 20
      4.2.3 Area-averaging technique 22
   4.3 Uncertainty quantification 23
   4.4 Area-averaged losses 24
5. Conclusions 28

References 30

Table of Figures

Figure 1. US electricity production by source, 2012. 1
Figure 2. Diagram of the Virginia Tech Transonic Tunnel facility. 7
Figure 3. View of the tunnel test section. 8
Figure 4. View of cascade "window" with blades. 9
Figure 5. View of cascade instrumentation. 9
Figure 6. Comparison of blade profiles. 10
Figure 7. Comparison of mean-line and near-tip profile blade loading at design incidence and an exit Mach number of 0.51. 13
Figure 8. Comparison of present study blade loading to that of Bakhtar et al. (1995). 14
Figure 9. Comparison of present study blade loading to that of Song et al. (2007). 14
Figure 10. Comparison of present study blade loading to that of Abraham et al. (2010). 15
Figure 11. Comparison of experimental and CFD blade loading for the mean-line profile at design incidence. 15
Figure 12. Variation of mean-line profile blade loading with incidence angle. 16
Figure 13. Comparison of mean-line profile blade loading at exit Mach numbers of 0.40, 0.51, and 0.60. 17
Figure 14. Incidence angle variation in the pitchwise direction for the mean-line profile at design incidence 18
Figure 15. Total pressure variation in the pitchwise direction for the mean-line profile at design incidence. 19
Figure 16. Inlet Mach number variation in the pitchwise direction for the mean-line profile at design incidence. 19
Figure 17. Relative inlet Mach number variation in the pitchwise direction for the mean-line profile at design incidence. 20
Figure 18. Example of local profile loss coefficient versus blade pitch. 21
Figure 19. CFD prediction of local loss coefficient (Nunes 2013). 22
Figure 20. Example of pitch definitions used to calculate area-averaged total pressure loss coefficient. 23
Figure 21. Area-averaged losses versus exit Mach number for mean-line profile, 0° incidence. 24
Figure 22. Area-averaged losses versus exit Mach number for mean-line profile, -6° incidence. 25
Figure 23. Area-averaged losses versus exit Mach number for mean-line profile, +4° incidence. 25
Figure 24. Area-averaged losses versus exit Mach number for the mean-line profile. 26
Figure 25. Area-averaged losses versus exit Mach number for the near-tip profile. 27

List of Tables

TABLE 1. BLADE PROFILE PARAMETERS. 11

1. Introduction

The importance of steam turbines to the quality of modern life is difficult to overestimate. Attempting to imagine the industrial revolution without this key technology is as impossible as it is nonsensical. Venerable though it may be, the steam turbine is by no means a relic. This crucial machinery still accomplishes well over half of US electricity production.

1.1 Steam turbine use

Figure 1 shows US electricity production in 2012. The left section of the figure shows the sources that traditionally rely on steam turbines. These sources account for almost 58% of the total electricity production. The section on the right shows sources that do not necessarily use steam turbines. It is certain, however, that steam turbines in combined cycle plants also accomplish some of the production listed under "natural gas."

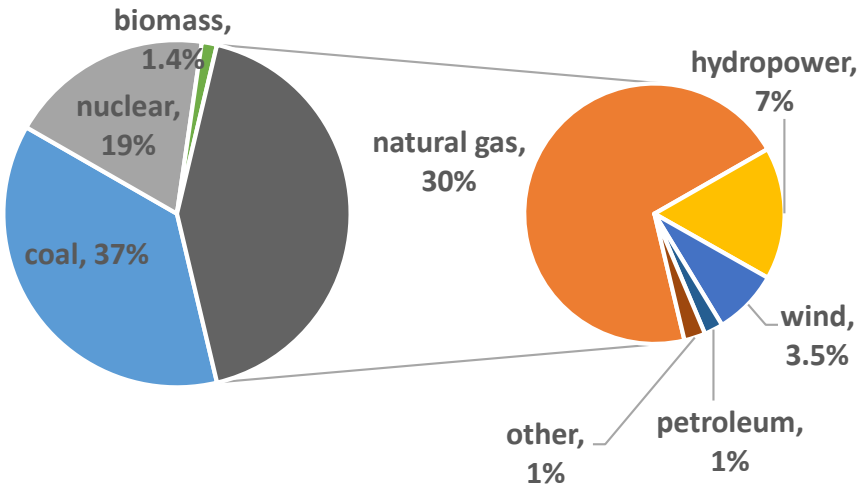

Figure 1. US electricity production by source, 2012.

These recent numbers show that the added natural gas capacity over the past decades has brought its share of the energy production on par with that of coal. The rise of gas turbines for large-scale power generation has rightfully consumed much of the economic, political, and academic interest over the past several decades. With the advent of the combined cycle plant, however, it is clear that the steam turbine is not a technology in decline.

1.2 Loss mechanisms

There is much value, then, in the study of methods to increase the efficiency of steam turbines. One may undertake this by reducing a number of different loss mechanisms. Ainley and Mathieson [1] identified four: profile, secondary, tip clearance, and annulus losses. These definitions are somewhat arbitrary. While one may reasonably separate "tip clearance" losses to analyze individually, the "annulus" and "secondary" categories are less defined, with the latter more often than not serving as a catchall for a variety of three-dimensional phenomena.

Ultimately, all loss mechanisms serve to increase entropy [2]. Whether this occurs in a vortical structure such as those caused by endwall effects, with the mixing of different gas streams, or by means of flow separation, there is a great benefit to understanding the nature of the loss. With the loss mechanisms well understood, the designer is in a better position to reduce its effects.

The best understood category of losses is likely profile losses. Most define these as the combination of several "two-dimensional" effects, namely those produced by the boundary layers (i.e. skin friction), trailing edge mixing, shock losses, and any flow separation from the blade surface. These effects lend themselves to experimental study in linear cascades such as the one used in the present study. The relative simplicity of this type of test compared to three-dimensional experiments means profile losses are more widely studied. The correlation of these experimental results is especially useful to turbine engineers as a tool to design new components.

1.3 Blade reaction

With respect to a turbine stage, the degree of reaction is a measure of where the pressure drop occurs [3]. Zero reaction is a scheme by which the pressure drops only across the stationary nozzles, with none occurring in the moving blades. The moving blades, then, are "impulsive"; they do not accelerate the flow, but only serve to change its direction. The relatively symmetric profile of these blades makes them appear somewhat like a bucket, a term used in some industries for this type of airfoil. Many steam turbine designs use one or several impulse or low-reaction stages at the front of the high-pressure turbine to quickly reduce pressure and extract large amounts of work [3].

Fifty percent reaction indicates a pressure drop shared equally by the stationary vanes and moving blades. The profiles of the vane and blade in this scheme are therefore more similar and may even be identical in some applications to reduce manufacturing costs. Higher-reaction stages are preferred in low pressure steam turbines and throughout gas turbines [4].

These statements are both general and qualitative. In reality, degree of reaction increases from the root to the tip of the blade. The method of satisfying radial equilibrium determines the specifics of the geometry [5].

The present study attempts to measure the profile losses of low-reaction, high-pressure steam turbine blades. Engineers at Elliott Group, the sponsoring organization, will then use the data to refine a propriety loss model for this type of blade.

2. Literature review

Both steam turbines and linear cascade tests have been around for many years, but there is an apparent dearth of modern study on profile losses of low-reaction, high-pressure steam turbine blades. That is not to say that much of the fundamental work on profile losses is inapplicable. In fact, many modern design tools are extensions of these venerable models.

2.1 Loss models

When Ainley and Mathieson [1] based their calculations on data from both gas and steam turbines of varying degrees of reaction, they created the most enduring model for estimating blade profile losses. A decade later, Horlock [6] also resolved to study both gas and steam turbines conjointly. Unfortunately, much of that data was several decades old at the time of his writing and measured only overall efficiencies. After another decade, an analysis by Craig and Cox [7] noted the inadequacy of Ainley and Mathieson [1] for current steam turbine design and proposed their own modifications. They claimed good agreement with a large amount of experimental data, but the source and type of such data was rather opaque.

The contemporary study of Dunham and Came [8] revisited the Ainley and Mathieson [1] model. They made use of additional gas turbine data taken in the intervening decades, a tradition carried on by Kacker and Okapuu [9] twelve years later. In each case, the investigators adjusted the model to reflect more closely "competent" modern gas turbine designs, but did not account for the design of steam turbines.

2.2 Application of loss models to modern blades

With the rise of effective computational techniques, loss models became one of many tools at the disposal of turbine designers. Researchers thus began to reexamine and critically asses the time-honored methods. Denton [2] offers an excellent discussion on the fundamental principles of loss mechanisms and describes how each company often tunes a loss model to reflect its own proprietary designs. He cautions that these tools are relatively ill suited to the design of radically new profiles as they may severely over-predict their losses.

Nevertheless, design processes remained more often specific than general. Of interest to the present study, Havakechian and Greim [10] presented an overview of the design process for 50% reaction steam turbine blades. Low-reaction blades see significantly less treatment in the literature. Wei [11] contributed one of the few studies to comment on the applicability of revised loss models to low-reaction blades. He stated that these tools tend to over-predict the losses of impulse stages, though he does credit the efforts of Craig and Cox [7] for developing the most applicable model. This result is encouraging to the present study, as it suggests that reviewing loss models in light of data from recent similar designs can make them more accurate.

2.3 Recent experiments on steam turbine airfoils

Thus, given sufficient experimental study of modern low-reaction steam turbine blading, one could attempt a further revision of a loss model to improve its prediction on those geometries. Unfortunately, there does not appear to be sufficient data in the open literature to do this. Bakhtar, Ebrahimi and Bamkole [12] performed a detailed cascade study of steam turbine blades, but used a high-reaction tip profile and were predominantly concerned with the effects of nucleating steam. Li, Chu, Yoo and Ng [13] investigated steam turbine nozzles in the Virginia Tech facility used in the current study, but again these results do not reflect a low-reaction blade. Another study in this facility conducted by Song, Ng, Cotroneo, Hofer and Siden [14] focused on low-solidity, low-pressure steam turbine blades.

Given the wealth of experience with loss models and their ease of use, it is safe to predict their continued utility in turbine blade design for many years to come. In the interest of accuracy, however, the designer must continually compare his predictions with recent experimental results of the same blade type. This study attempts to provide some of this necessary data for a modern low-reaction high-pressure steam turbine blade.

3. Experimental setup

Axial flow steam turbines feature a radial array of blades about a rotating shaft. A great deal of the complexity in these machines lies in the fabrication and assembly of this structure. In testing the components, one would desire to simplify this construction while preserving the features on which the fundamental physics depend. For the measurement of profile losses of turbine blades (largely considered a two-dimensional effect), one simplification is the transformation of the radial geometry to a planar experiment. The "unrolling' of a blade row onto a plane creates a linear cascade. Since the blade profile often varies from hub to tip, one must decide which section of the blade to test. Often, one is concerned with the mean-line of the blade, though sections of the blade hub and tip are also instructive.

A further experimental simplification is the reduction of the overall blade count to decrease the length of the cascade. In the absence of inlet distortions, the conditions of an actual turbine tend to have a high degree of circumferential uniformity. By the nature of its geometry, a linear cascade of finite length will not achieve perfect periodicity of flow conditions along the cascade due to the end effects. Thus, the experimental design must strive to control these deficiencies by isolating the flow nonuniformity to the ends of the cascade to keep such effects away from areas in which one is to take valid data.

3.1 Virginia Tech Transonic Tunnel

The Virginia Tech Transonic Tunnel has been home to this type of experiment for many years. As shown in Figure 2, the tunnel is a blowdown type, in which a four-cylinder reciprocating compressor creates a reservoir of compressed air in a tank before each test. Many types of experiments performed in the facility make use of a traversing scheme to obtain the maximum amount of data in each tunnel run. In these scenarios, it is desirable to maintain constant tunnel conditions for the duration of the traverse. A butterfly valve subject to active control serves this purpose. The investigator sets a desired condition that the valve will work to maintain provided a sufficient reservoir of compressed air remains.

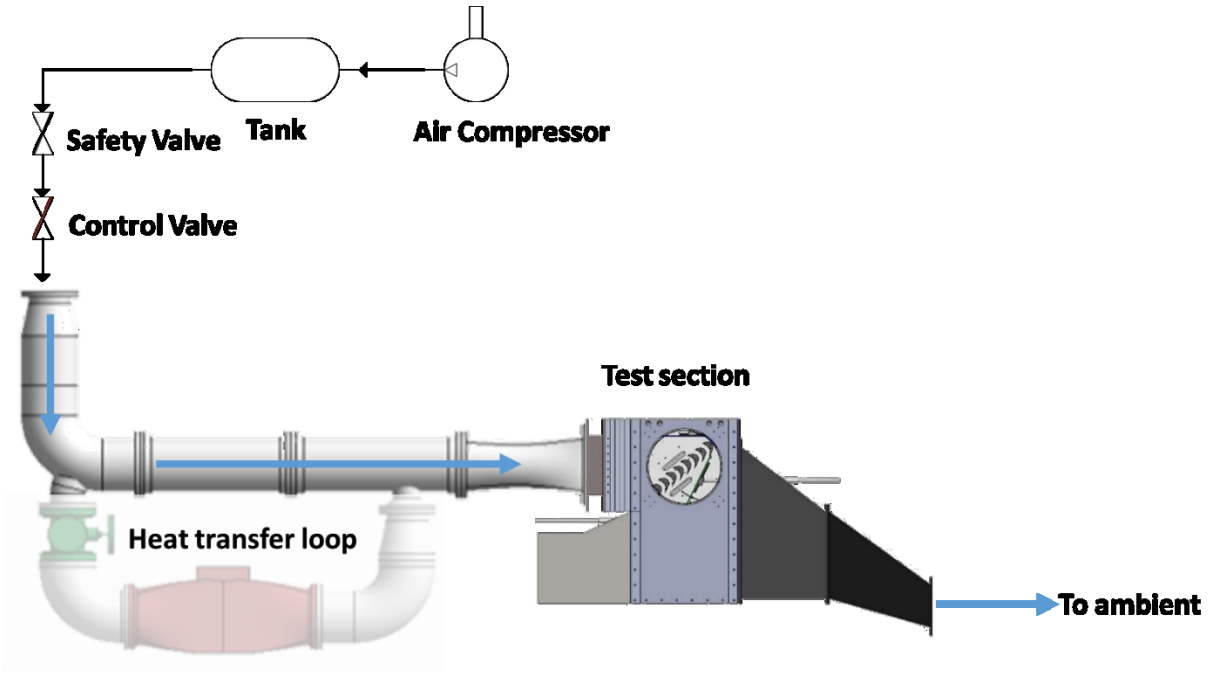

Figure 2. Diagram of the Virginia Tech Transonic Tunnel facility.

Figure 3 shows a closer look at the flowpath in the test section. After a pipe delivers flow from the storage tank to the test section, the tunnel transitions to a rectangular cross-section. The flow develops and passes through a turbulence grid. A hot-wire anemometer placed 44.5 cm (17.5 in) away from the grid and at the center of the measurement region measured a turbulence intensity of 5% and a turbulent length scale of 1.5 cm (0.59 in).

One notes that when the profiles tested in the facility are blades with a high degree of turning, the flow exiting the blade row must execute a circuitous path to the tunnel outlet. The presence of a large plenum downstream of the blade exit is an attempt to mitigate this factor. Nevertheless, the flow will still tend toward the low-pressure outlet and there is a potential for the downstream measurements to experience adverse effects such as non-physical flow angles.

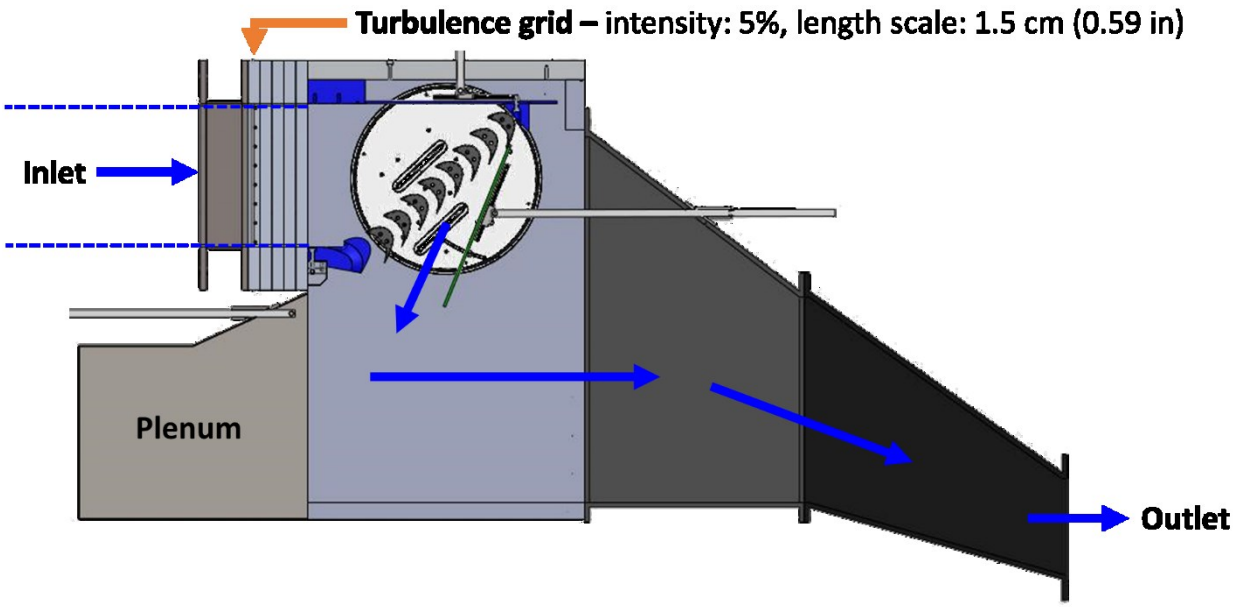

Figure 3. View of the tunnel test section.

One feature of the cascade that aims to reduce this effect is the tailboard, as shown in Figure 4. It attempts to keep the flow exiting the blades in streamlines determined by the geometry of the blades and the flow velocity. The tailboard pictured is roughly twice the length of the one used in the preliminary testing. After the downstream angle measurements from those tests showed that the flow was "peeling off" toward the outlet, it revealed the necessity of more effective control of the downstream flow.

The headboard is an upstream flow-control tool. Though designed to allow variation of its angle with respect to the mainstream flow, this study maintained its angle parallel to the flow. A movable wedge attached to the headboard allowed control of the gap between the top of the test section and the uppermost blade. This was especially important so as not to open a large gap at positive incidence angles.

At the other end of the cascade was the bottom block, which aimed to increase periodicity by controlling the flow below the bottom blade. This component was interchangeable to adapt to varying cascade incidence angles. Figure 4 shows the bottom block used for a design-case incidence. This block actually served as an additional blade over most of the span, as it used the blade same blade profile as the rest of the cascade and featured and internal passage with only the edges remaining solid for support. A fused deposition modeling (FDM) printer allowed the construction of these parts from ABS plastic.

Rotation of the "windows" on which the blades were mounted set the incidence angle. These two circular components were made of clear polycarbonate, with blades placed between them and affixed with steel dowel pins. As Figure 4 indicates, rotating the windows clockwise tended to make the incoming flow see more of the blade pressure side, thus creating positive incidence. Rotating the windows counter-clockwise tested a negative incidence condition.

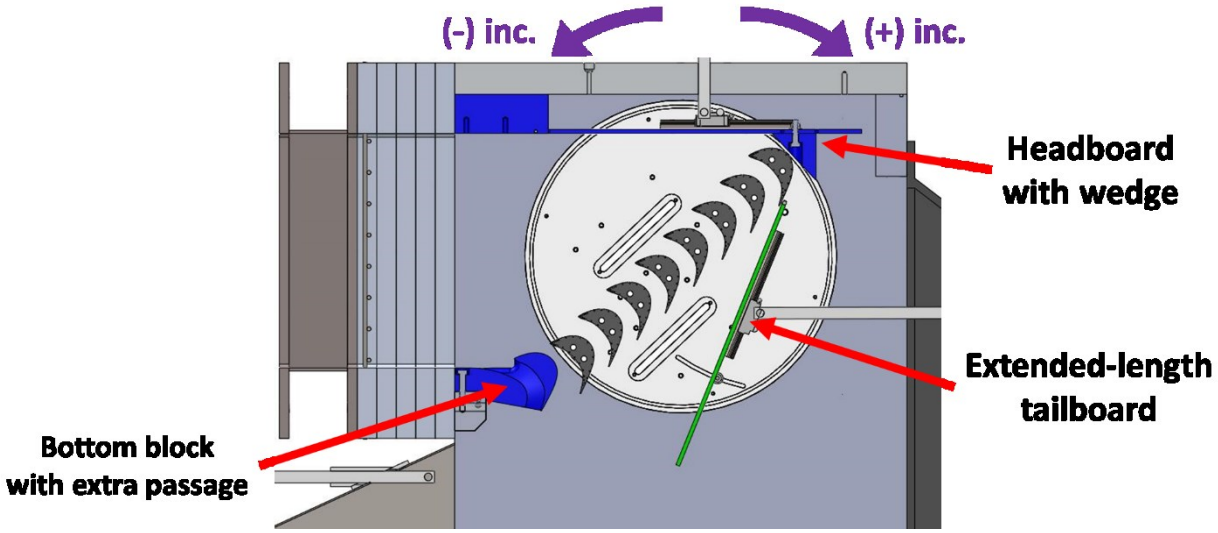

Figure 4. View of cascade "window" with blades.

3.2 Upstream and downstream instrumentation

Measurement of profile losses requires information about the flow entering and exiting the blades. As shown in Figure 5, the upstream measurement station was located at $0.5*C_{ax}$ from the blade leading edge, where C_{ax} denotes the blade axial chord. At this location, a fixed Pitot static probe measured both total and static pressure. Additional static pressure information was available from eleven wall taps. An alternative configuration for measuring upstream conditions omitted the fixed Pitot static probe in favor of a traversing five-hole probe.

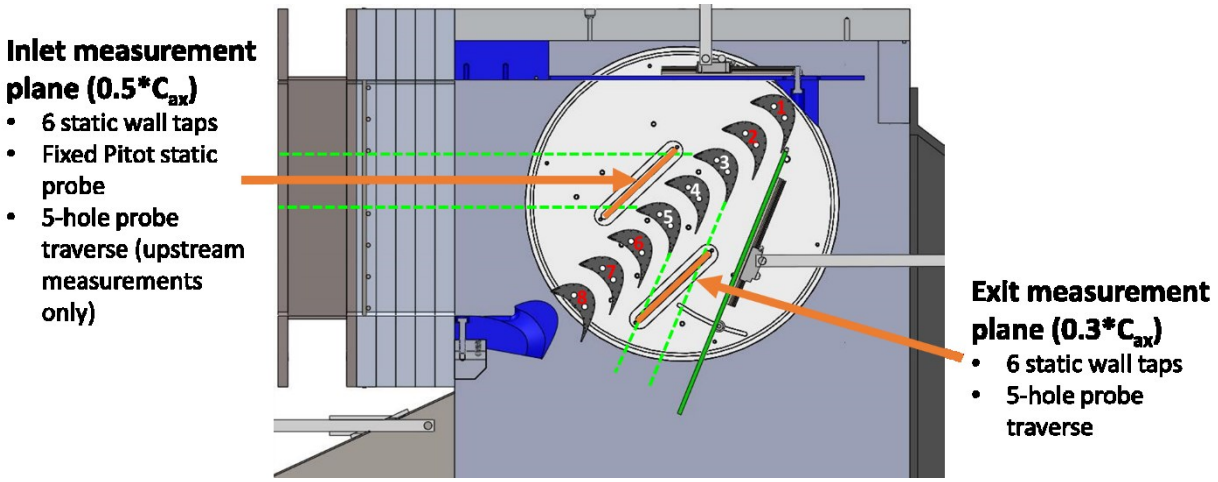

Figure 5. View of cascade instrumentation.

The measurement slot was 15.24 cm (6 in) long. With a blade pitch of 6.35 cm (2.5 in), this allowed measurements over more than two full pitches. The exit measurement station was $0.3*C_{ax}$ downstream from of the blade trailing edge. It also featured 11 wall static pressure taps and a 15.24 cm (6 in) slot for traversing the five-hole probe. It was in this configuration,

with the five-hole probe mounted downstream, that provided the spatially varying data useful in determining the profile loss coefficient.

3.3 Blade profiles

The two blade profiles investigated were from the mean-line and near-tip sections of the same low-reaction, high-pressure steam turbine blade. Unlike many gas turbine blades, these steam turbine blades did not exhibit a large variation in profile ("twist") from hub to tip, as evinced by the similarity of the profiles in Figure 6.

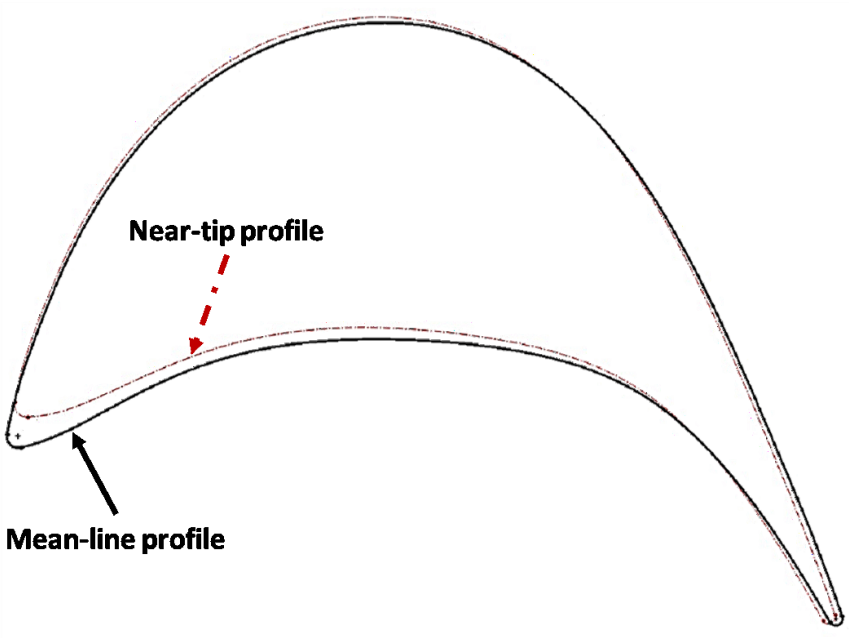

Figure 6. Comparison of blade profiles.

The blade profiles show a high degree of symmetry and a sharp leading edge relative to high-reaction blades. They are also noticeably "thicker" with respect to their pitch than gas turbine profiles and thus constitute a higher blockage to the flow. This, combined with their designed lack of acceleration, meant that achieving high exit Mach numbers was difficult. Ultimately, the search for higher exit Mach numbers brought the testing close to the facility safety limit. Thus, the highest exit Mach numbers achieved were near 0.6.

The scaling parameter for the profiles was the blade pitch. This required scaling down each profile approximately 30% until their pitch was 6.35 cm (2.5 in). The blades differ mainly at the leading edge, with the inlet angle of the mean-line profile being 43.3° and that of the near-tip profile 50.0°. This was the main driver in the lower blade turning of the near-tip profile, since the profiles are very similar at the trailing edge.

Table 1 summarizes other parameters of interest.

Table 1. Blade profile parameters.

Parameter	Mean-line	Near-tip
original pitch (in)	3.23	3.29
scaled pitch (in)	**2.50**	**2.50**
scaled true chord (in)	3.74	3.71
scaled axial chard (in)	3.68	3.62
inlet angle (°)	43.3	50.0
exit angle (°)	24.5	24.0
turning (°)	112.2	106.0
# PS static press. taps	12	11
# SS static press. taps	15+LE	16+LE

3.4 Blade loading instrumentation

This experiment included more blade loading measurements than any previously performed in the facility. Data from these taps allowed visualization of blade loading on the same section of the cascade measured by the traversing slots. An important consideration in sizing the blades was the feasible measurement density at the leading and trailing edges.

Parts of three blades bounded the two passages of interest. These included both the pressure- and suction-side of a central blade along with adjacent pressure- and suction-sides of two additional blades. Each leading edge also contained a static pressure tap. Table 1 lists the number of taps for each profile. Both designs had measurements over approximately 90% of the axial chord, with the small thickness of the trailing edges preventing measurements farther aft.

Simultaneous measurement of all these pressures required the use of two pressure-scanning systems totaling 80 ports. A single LabVIEW instrument managed the synchronization and data collection as well as the command of the traversing mechanism and the valve control.

4. Results and discussion

4.1 Blade loading

An important part of many cascade tests is a thorough analysis of the blade loading. This study found that the blade loading was similar between the two profiles, but different from results published in the open literature. The match with CFD results was remarkably close.

4.1.1 Blade loading equations

Two common methods of expressing blade loading are the pressure ratio and the isentropic Mach number on the blade surface, usually as a function of axial chord. The present study uses the pressure ratio definition

$$p_{ratio} = \frac{p_{surf}}{p_{t,in}}, \tag{1}$$

where p_{surf} is some local static pressure measured by the taps on the blade surface and $p_{t,in}$ is the total pressure measured by the upstream Pitot probe. Alternatively, the isentropic Mach number

$$M_{isen} = \sqrt{\frac{2}{\gamma - 1}\left[\left(\frac{p_{t,in}}{p_{surf}}\right)^{\frac{\gamma-1}{\gamma}} - 1\right]} \tag{2}$$

provides the same information (note the inverse of the ratio previously described). Here, the pressure definitions are the same as in the pressure ratio. The ratio of specific heats is γ, which this study always takes to be 1.4.

4.1.2 Comparison of experimental blade loading

Since the experiment gathered information from two pressure sides and two suction sides, the blade loading can also serve as an indication of the flow periodicity through the passages of interest. In the following plots, there are two measurements at every axial location. Often, they are coincident, indicating that the flow was nearly identical in the passages. When the points appear more distinctly, it indicates less periodic flow.

Of primary concern is the existence of any differences in blade loading between the profiles tested. Since a geometric comparison of the profiles showed only small differences at the leading edge, one would expect that the blade loading would be show a similar trend. Indeed, Figure 7 indicates that the blade loading at the design incidence and at an exit Mach number of 0.51, the profiles perform similarly. They both exhibit a “crossover” or “unloading” over the first 15% of the axial chord. Also notable is the complex curvature of the loading on the pressure side of the blade whereby the blades are more highly loaded at 30% and 70% axial chord than at 50%.

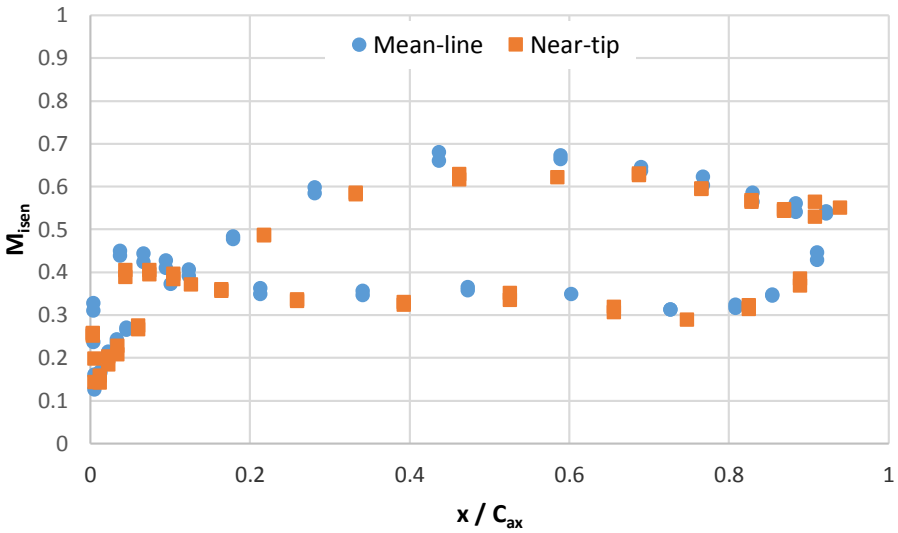

Figure 7. Comparison of mean-line and near-tip profile blade loading at design incidence and an exit Mach number of 0.51.

The near-tip profile shows slightly higher loading on the leading edge of the pressure side and along the middle of the suction side, but is otherwise very similar to the mean-line profile. Both profiles are extremely "flat," as one might expect since low-reaction blades do not drastically accelerate the flow. The similarity of the blade profiles in both geometry and loading suggests that additional comparisons are likely to be duplicative. This study will use the blade loading from the mean-line geometry for further comparisons.

4.1.3 Comparison of blade loading with open literature

Having established some of the unique features of the loading for this blade, it is now instructive to compare this loading with that of blades in the open literature. The work of Bakhtar, Ebrahimi and Webb [15] on a steam turbine rotor tip section used a very different blade geometry from the present study. Figure 8 shows that the blade loading is also very different. Their blade clearly has a much higher reaction, as evinced by the downward-sloping trend toward the trailing edge. Though there are no pressure measurements near the leading edge, the trend of the data shown does not indicate any "unloading."

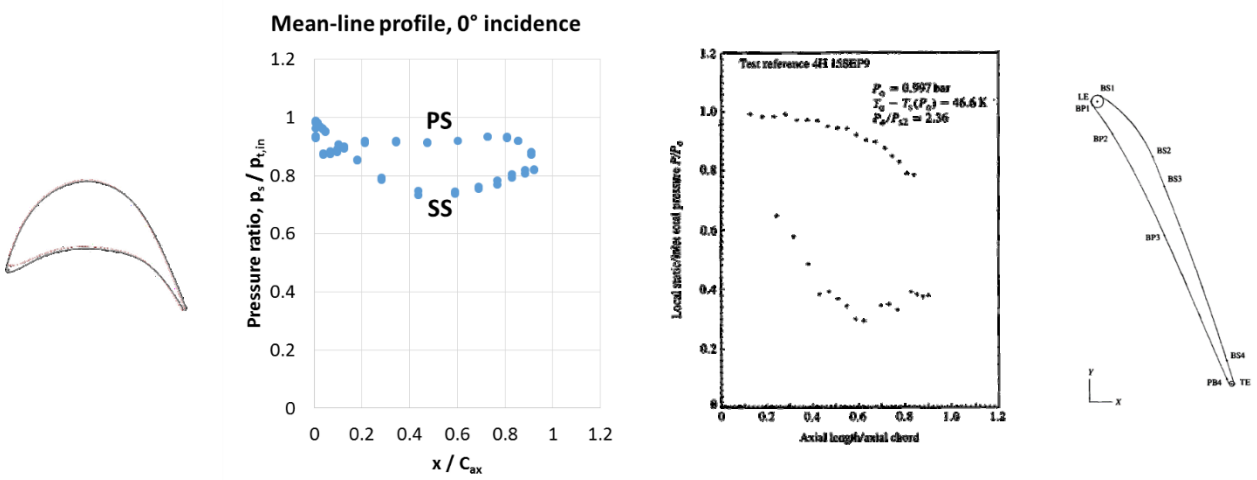

Figure 8. Comparison of present study blade loading to that of Bakhtar et al. (1995).

The comparison of the blade loading to that of the steam turbine nozzle studied by Song, Ng, Cotroneo, Hofer and Siden [14] does not find a closer match. Again, the key features of "unloading" at the leading edge and a lack of acceleration through the blade row are not present, as shown in Figure 9. It is clear that the steam turbine nozzle is a much higher reaction design than the blade profile in the present study.

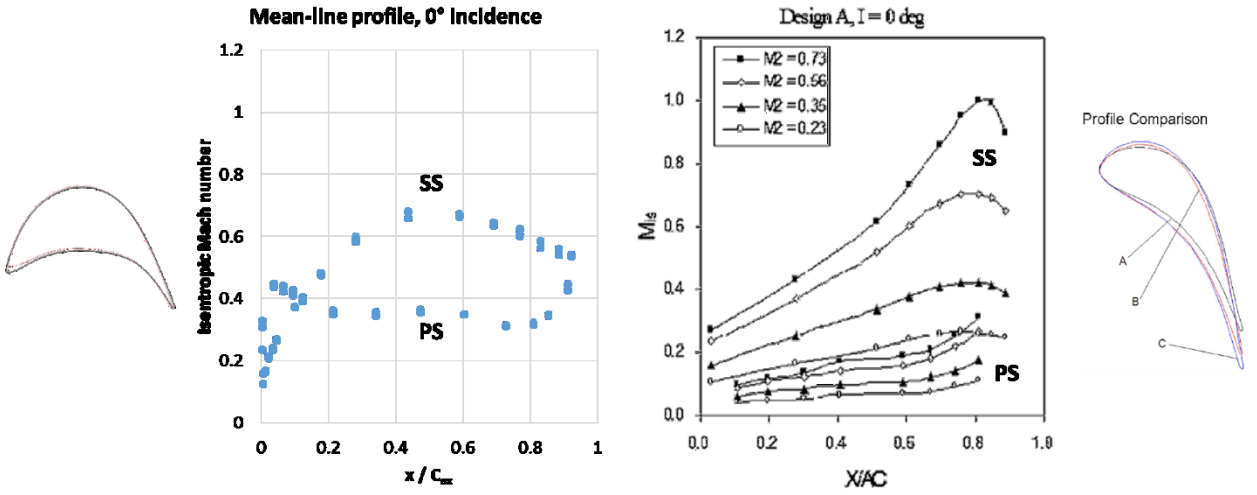

Figure 9. Comparison of present study blade loading to that of Song et al. (2007).

Interestingly, the blade loading is slightly more similar to the gas turbine blade studied by Abraham, Panchal, Xue, Ekkad, Ng, Brown and Malandra [16] in the same Virginia Tech facility used for this experiment. While obviously still lacking the defining features, Figure 10 shows the overall shape of the distributions is more similar. This is perhaps due to the high degree of turning imparted by both blades.

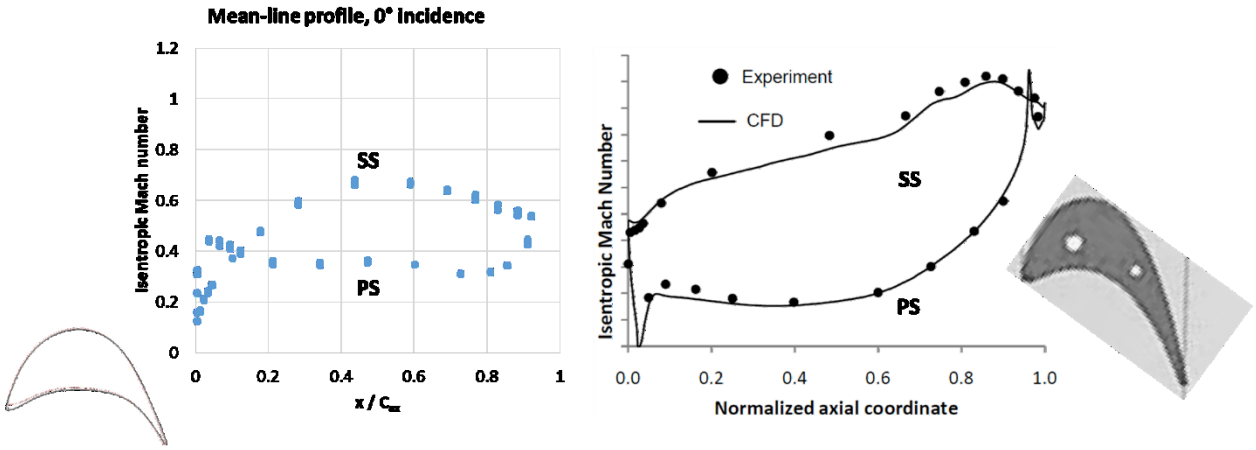

Figure 10. Comparison of present study blade loading to that of Abraham et al. (2010).

4.1.4 Comparison of blade loading with CFD results

Having established that this blade exhibits loading distributions very different from most airfoils in the open literature, one may now begin comparisons with other relevant data. One important comparison is with available data from CFD. Nunes [17] performed a thorough computational analysis on this blade as a part of the present study. Figure 11 shows a comparison of the experimental blade loading with the results from CFD. The incidence angle is zero for both cases, but there was a difference of about 0.03 in exit Mach number. Using a linear interpolation of the CFD results allows some comparison of the blade loading.

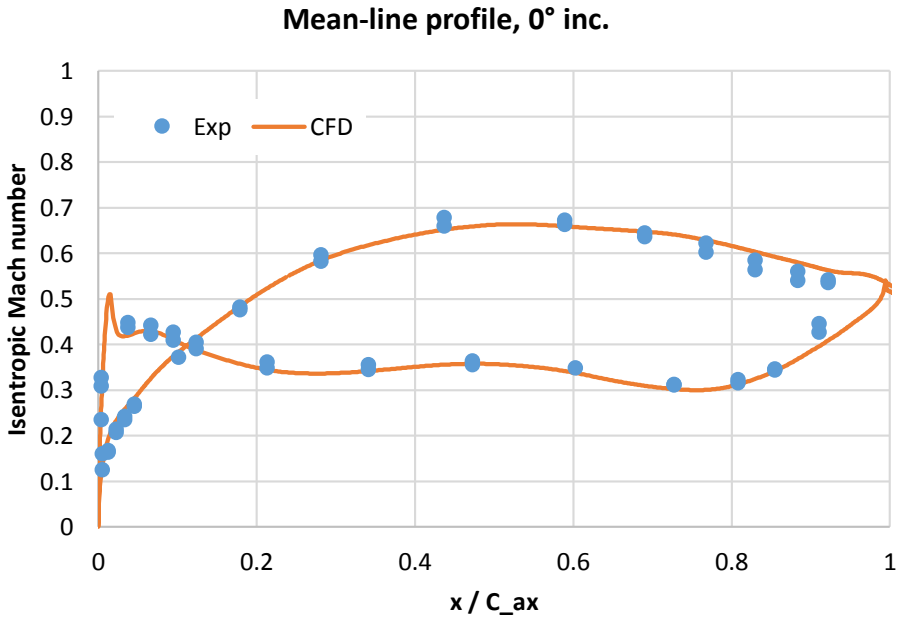

Figure 11. Comparison of experimental and CFD blade loading for the mean-line profile at design incidence.

The agreement between the experimental and computational blade loading is quite good. Both sets of data agree on major features such as leading edge "unloading" and curvature on the pressure side. The largest difference occurs on the suction side trailing edge.

4.1.5 Effect of incidence angle on blade loading

Figure 12 shows the effect of incidence angle on blade loading for the mean-line profile. The experiment showed very little change in blade loading over the ten-degree incidence swing. A rudimentary numerical integration of the experimental results showed a 6% loading increase when moving from design incidence to -6° incidence. Moving from design to +4° incidence only increased blade loading by 3%. These small changes are due to the virtually identical results over the aft 20% of axial chord. The only discernable change is in the suction side leading edge loading.

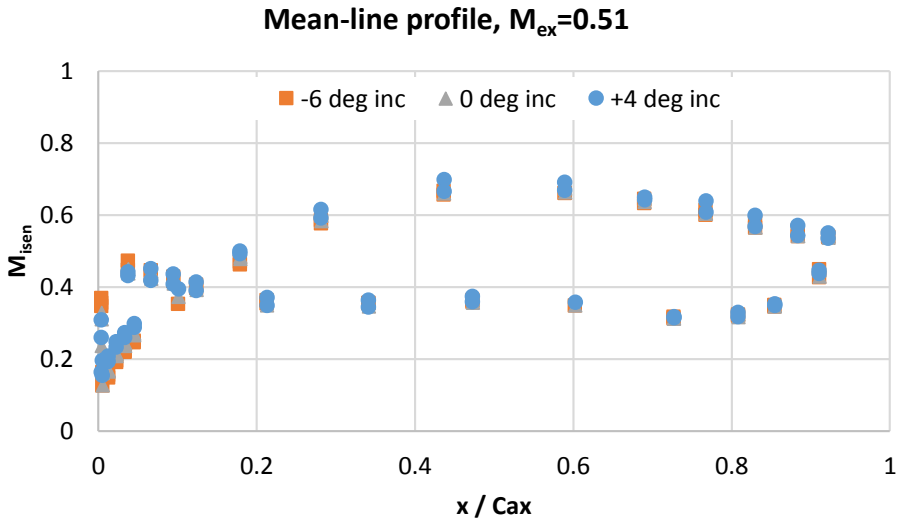

Figure 12. Variation of mean-line profile blade loading with incidence angle.

4.1.6 Effect of exit Mach number on blade loading

The other major parameter this study explored was exit Mach number. Figure 13 indicates that the blade loading does not change qualitatively as one increases the exit Mach number from 0.4 to 0.6. Interestingly, there are enough measurements at the trailing edge of the blade to estimate the exit Mach number directly from the blade loading data.

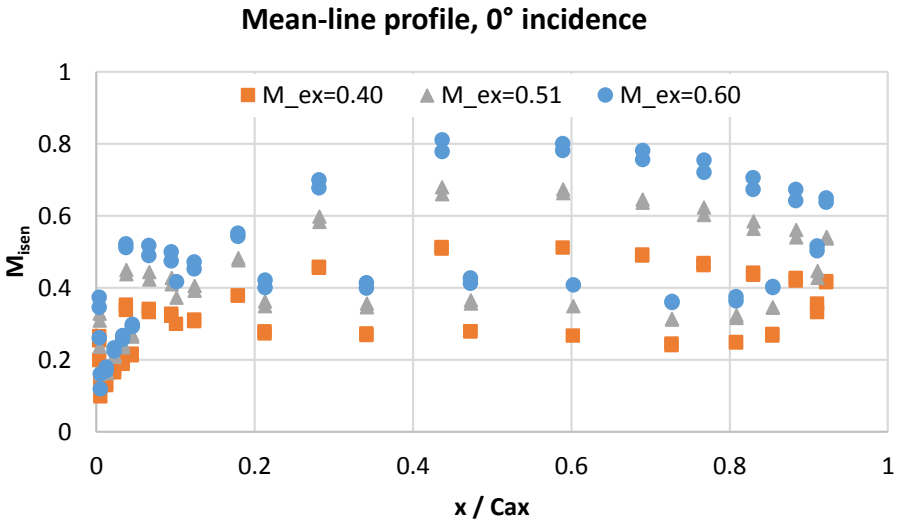

Figure 13. Comparison of mean-line profile blade loading at exit Mach numbers of 0.40, 0.51, and 0.60.

The blade loading presented here serves to describe the major trends seen in the data; it is by no means an exhaustive catalog. Throughout the experiments, monitoring the blade loading of every tunnel run helped establish flow conditions and periodicity of the measured passages.

4.2 Traverse measurements

One may draw many conclusions from the blade loading data, but to obtain detailed information about the entire flow field, an investigator needs additional measurements at different spatial locations. The present studied relied heavily on a traversing five-hole probe to provide this information. The combination of data from this instrument with additional total and static pressure information from stationary probes allows a detailed look at the flow before and after the blade row.

4.2.1 Upstream traverse measurements

Measuring the upstream flow required only placing the five-hole probe at the appropriate location. This experiment placed all upstream measurements at $0.5*C_{ax}$ from the blade leading edge. One important check of the upstream traverse data is the uniformity of the inlet flow angle. Unfortunately, there was no direct access to the five-hole probe tip at the upstream location, meaning the only way to determine the relationship between the orientation of the probe and its surroundings was by eye. While this means the angle values measured by the probe incur a significant amount of uncertainty, the comparison of the experimental blade loading to CFD has already shown that the effective incidence must be very close to zero. What the upstream five-hole did, then, is investigate any spatial variations in this inlet flow that may contribute to aperiodicity in the blade passages.

Figure 14 shows the variation of effective incidence angle with the mean-line profile blades installed at their design incidence. In this configuration, the angle variation is less than ±1° across the measured region. Rotating the cascade to off-design incidence angles can alter this variation somewhat due to changes in tunnel flowpath, but the observed variation at all conditions was within ±2°. This variation does not appear sensitive to exit Mach number. The exit Mach numbers used here are approximate since there was not sufficient downstream instrumentation to measure it in this configuration. Instead, tunnel controls were set to identical values of runs that previously produced the given exit Mach number.

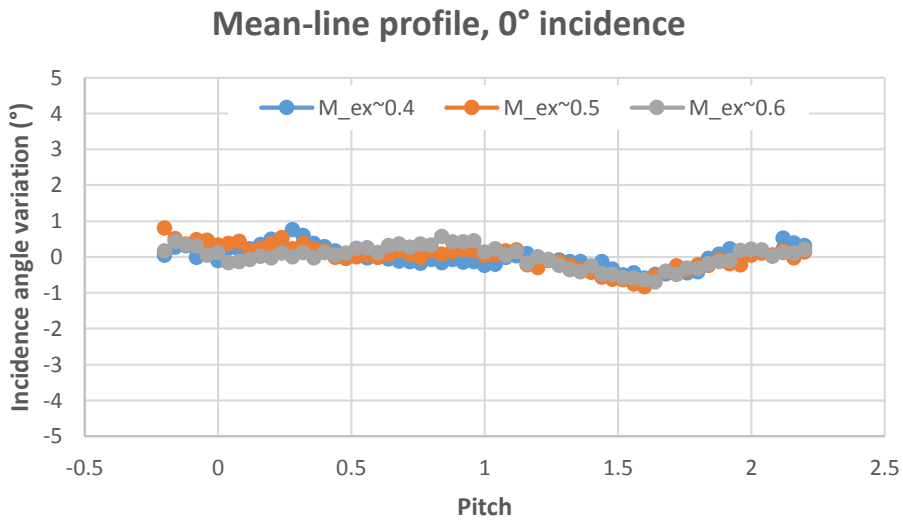

Figure 14. Incidence angle variation in the pitchwise direction for the mean-line profile at design incidence

Other factors besides the flow angles can affect periodicity, especially variations in total pressure. Figure 15 shows that the variations in total pressure are within ±1% for the mean-line profile, design incidence case. Analysis of the near-tip and off-design cases indicates that the variability of total pressure does not exceed ±1% in this study. As with the flow angle, the variation in total pressure does not appear sensitive to exit Mach number over the range 0.3 to 0.6. There appears to be a periodic trend to the variation, but it does not match the spacing of the blades, rather, it is similar to the spacing of the bars of the upstream turbulence grid, meaning the variation is likely due to vestiges of the wakes created at that location.

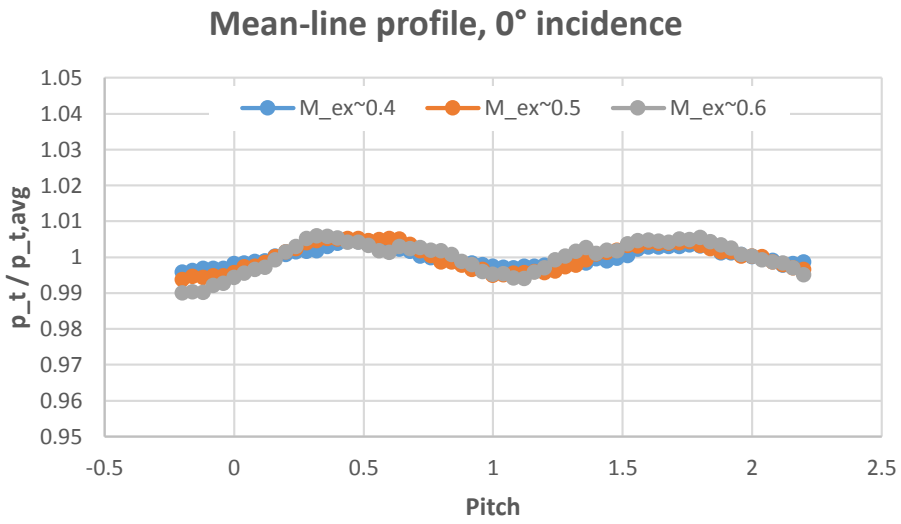

Figure 15. Total pressure variation in the pitchwise direction for the mean-line profile at design incidence.

The variation in inlet total pressure manifests itself in an inlet Mach number variation as well. This is perhaps a better way of describing the variation, as this study references flow conditions to exit Mach number. In Figure 16, one can see the inlet Mach number variation in absolute terms. This variation is less than ±0.02 for all cases. Taken as a percentage, however, this variation can be up to ±10%, as indicated by Figure 17. While at first this may seem like a large variation, it is still small considering the dominant effect of the downstream wake from the blades on the exit Mach number and the study references the average exit Mach number moving forward.

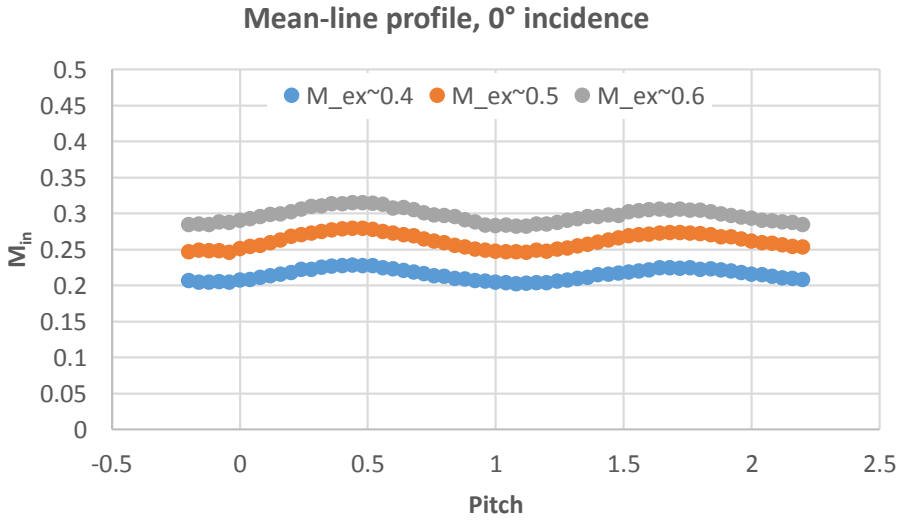

Figure 16. Inlet Mach number variation in the pitchwise direction for the mean-line profile at design incidence.

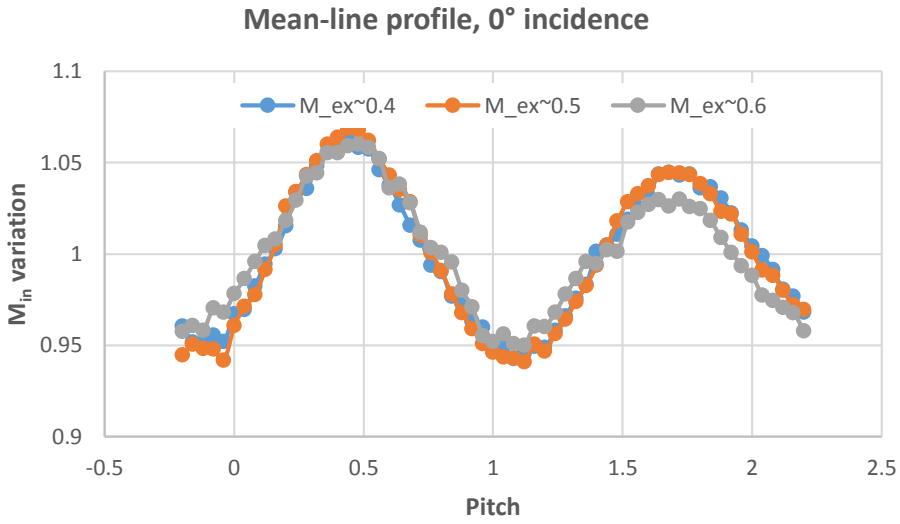

Figure 17. Relative inlet Mach number variation in the pitchwise direction for the mean-line profile at design incidence.

4.2.2 Downstream traverse measurements

After performing a characterization of the upstream flow, one may progress to the desired outcome of the study: determination of the profile loss coefficient. This investigation uses the common definition thereof:

$$Y = \frac{p_{t,in} - p_{t,ex}}{p_{t,ex} - p_{s,ex}} = \frac{total\ pressure\ loss}{exit\ dynamic\ pressure} \tag{3}$$

In this definition, one can see that the major concern is with the deficit of total pressure at the exit of the blade row. The exit dynamic pressure is a normalizing parameter.

In the present study, the inlet total pressure, $p_{t,in}$, is that measured by the fixed Pitot static probe located 0.5*C_{ax} upstream. Here, one assumes that the upstream total pressure does not vary spatially. This is reasonable since Figure 15 indicated the upstream total pressure variation was less than ±1%. While the control valve attempts to preserve constant conditions in the tunnel throughout the duration of the traverse, keeping the temporally varying data from the upstream Pitot probe helps to correct for any small variations.

The traversing downstream five-hole probe measures the exit total pressure, $p_{t,ex}$. Here, a data reduction scheme takes the five pressure measurements, compares them with a calibration database, and outputs the total pressure. These data are both spatially- and temporally-variant, as one would expect from a traversing probe. This is the key measurement for determining the profile loss.

The final parameter affecting the profile loss coefficient is the exit static pressure, $p_{s,ex}$. This study used the average of the static pressures measured by six taps in the window at the same 0.3*C_{ax} location measured by the five-hole probe. There was very little spatial variation

in the exit static pressure, so the averaging served mainly to increase the precision of the measurement.

Combining these measurements, one may compute the local profile loss coefficient versus the blade pitch as shown in Figure 18. The traversing five-hole probe moves from the bottom to the top of the measurement location (from pressure-side to suction-side of the blades) taking data over 2.4 blade pitches. The regions of high losses are those in the blade wakes, directly downstream of the trailing edge. Areas between the blades show very low losses and this region is often termed an "inviscid core."

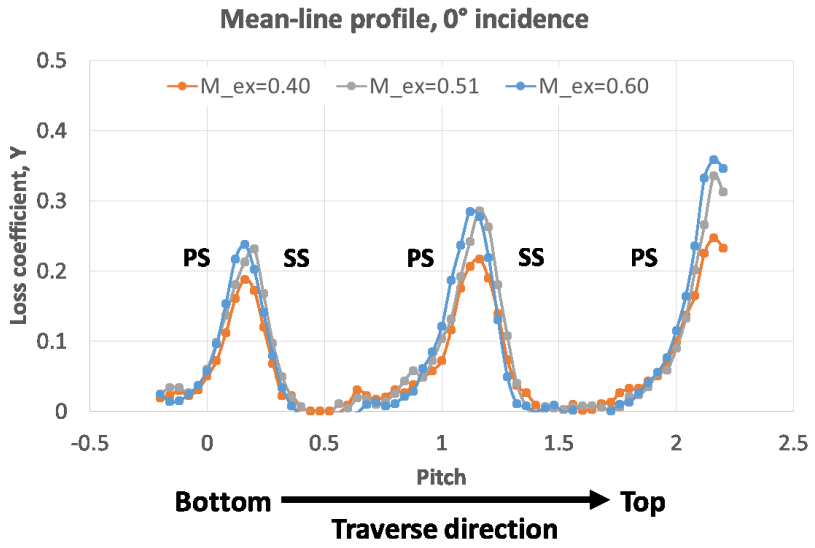

Figure 18. Example of local profile loss coefficient versus blade pitch.

Figure 18 also shows loss peaks that increase in magnitude with increasing exit Mach number, especially from 0.40 to 0.51. The CFD predictions of Nunes [17] do not indicate a similar phenomenon. Instead, Figure 19 shows very little change in the magnitude of the loss peaks, but does show a narrowing of the wakes with increasing exit Mach number. Averaging of this data allows quantification of these observations.

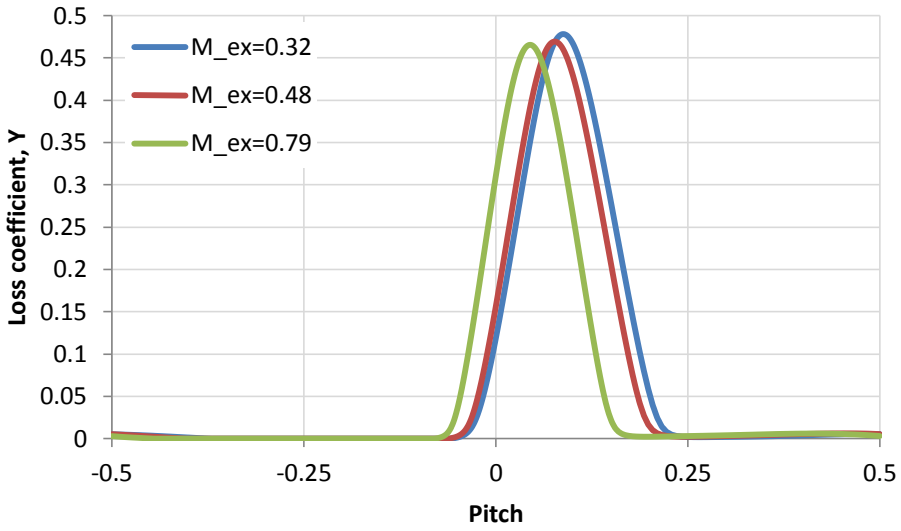

Figure 19. CFD prediction of local loss coefficient (Nunes 2013).

4.2.3 Area-averaging technique

An undesirable conclusion one may draw from the loss peaks in Figure 18 is the apparent aperiodicity of the flow. Periodic conditions would see the loss peaks constant with blade pitch, yet these results show a discernable upward trend as the traverse moves to the top of the measured area. As discussed previously, gaps at the top and bottom of the cascade and issues with the tunnel flowpath likely contribute to this aperiodicity. Nevertheless, the significant efforts taken to reduce these effects did not completely resolve the issues.

While undesirable as a source of uncertainty, the aperiodicity does not mean the data are useless. One may simply quantify the uncertainty due to the effect by carefully constructing the intervals over which one calculates the area-average loss coefficient. This calculation was necessary anyway as a quantitative measure of the profile losses.

A simple way to determine the area-averaged loss is to calculate the average total pressure loss coefficient over any integer number of pitches. This experiment measured data over 2.4 pitches. If one takes the data from the middle two pitches to eliminate any effects of the traverse accelerating or decelerating, the result is an area-averaged total pressure loss coefficient for the measured portion of the cascade. This is the interval from 0 to 2 pitches shown in Figure 20. One may also calculate the area-average using only the first or second pitches.

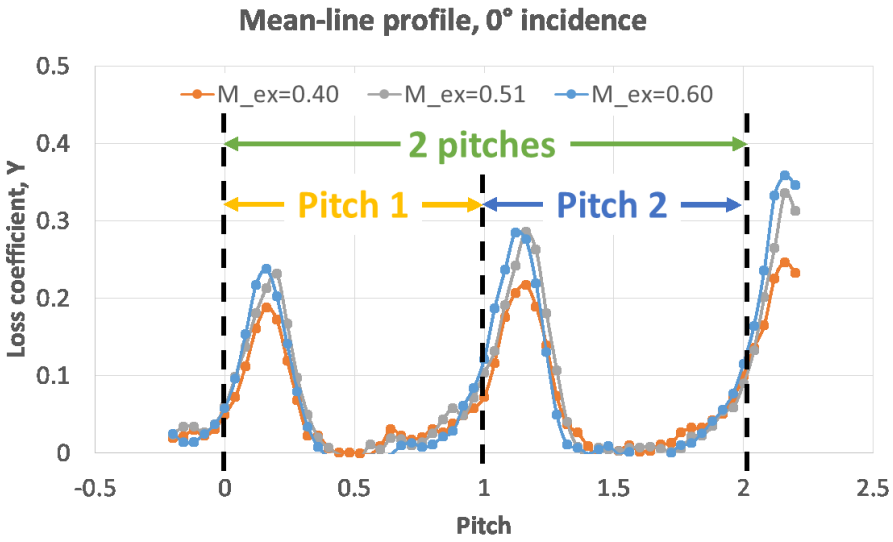

Figure 20. Example of pitch definitions used to calculate area-averaged total pressure loss coefficient.

One may use these averages to express the area-averaged loss coefficient with an associated uncertainty exclusively due to aperiodicity:

$$Y_{avg} = Y_{2-pitch\ avg} \pm \left| Y_{2-pitch\ avg} - Y_{1-pitch\ avg} \right|. \tag{4}$$

The absolute value of the difference between the two-pitch average and either one-pitch average will be identical, so the choice of using "Pitch 1" or "Pitch 2" is arbitrary.

4.3 Uncertainty quantification

One must also account for additional uncertainty due to the cascade instrumentation. For the single measures of area-averaged loss coefficient of interest in this study, Kline and McClintock [18] offer a convenient method for calculating the experimental uncertainty. Applying the appropriate equations yields an expression for the uncertainty of the loss coefficient:

$$w_Y = \left[\left(\frac{1}{p_{t,ex} - p_{s,ex}} w_{p_{t,in}} \right)^2 + \left(\frac{-(1+Y)}{p_{t,ex} - p_{s,ex}} w_{p_{t,ex}} \right)^2 + \left(\frac{Y}{p_{t,ex} - p_{s,ex}} w_{p_{s,ex}} \right)^2 \right]^{\frac{1}{2}}. \tag{5}$$

Since similar equipment measured all pressures, the instrument error of the system determines the uncertainty values (w). The uncertainty for the pressure scanning system is 0.05% of the full scale of 20 psi, thus each w = ±0.01 psi.

The loss coefficient uncertainty is also dependent on the relevant pressures. Though perhaps not obvious at first glance, the numerical result is a higher uncertainty at lower values of the loss coefficient. At the low exit Mach number of 0.4, this uncertainty can be over 10% of the

loss coefficient value. It is closer to 4% at the high exit Mach number of 0.6. The subsequent plots of the area-averaged loss coefficient show error bars with combined uncertainty. This is the sum of the uncertainty calculated with this analysis and the uncertainty from aperiodicity.

4.4 Area-averaged losses

With a prescribed method of assessing the area-averaged profile losses and uncertainties, the next step is to compare these results across profiles, incidence angles, and Mach numbers.

Starting with the latter, one notes in Figure 21 that for the design incidence, losses increase with exit Mach number over the range tested. This is contrary to the slight decreasing trend predicted by CFD, though the two match very well at low Mach numbers. As one can see from the wake profiles in Figure 19, the decreasing trend is the result of narrowing of the blade wakes with increasing exit Mach number.

The discrepancy between experimental and computational results represents about a 30% difference at the highest experimental Mach number. Still noteworthy, however, are the low overall losses; no measurements or calculations put the losses over 0.1 for the exit Mach number range of interest.

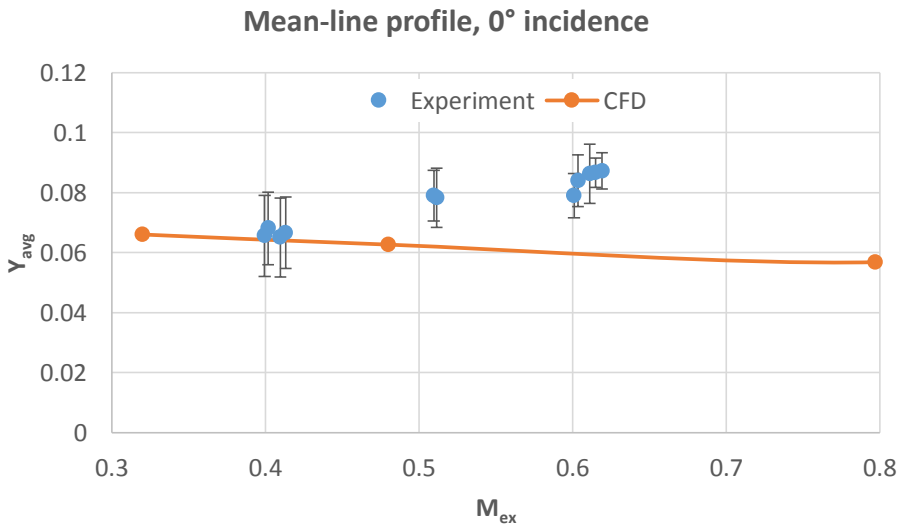

Figure 21. Area-averaged losses versus exit Mach number for mean-line profile, 0° incidence.

The off-design values show similar loss levels and trends. Figure 22 shows the experimental and computational results for the mean-line profile at -6° incidence. Figure 23 shows the same for +4° incidence. The negative incidence angle case is a more favorable experiment from a geometric standpoint since it tends to reduce the flow over the top of the cascade and ease the exit flowpath. This manifests in a smaller uncertainty due to aperiodicity for these

measurements. Additionally, the dependence of the average loss coefficient on the exit Mach number appears reduced, but the data still do not follow the trend of the CFD results. Conversely, tests at positive incidence show greater aperiodicity. Here, the trend of increasing losses with exit Mach number is similar to that shown by the design incidence.

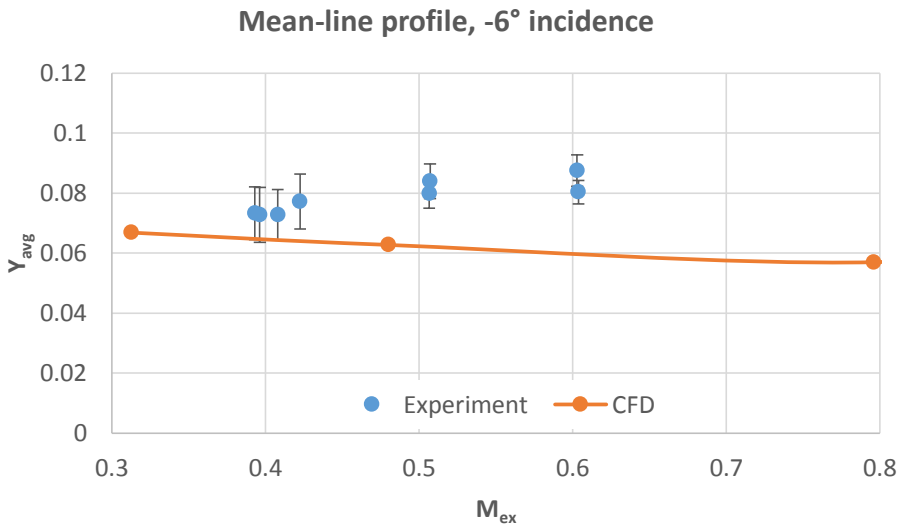

Figure 22. Area-averaged losses versus exit Mach number for mean-line profile, -6° incidence.

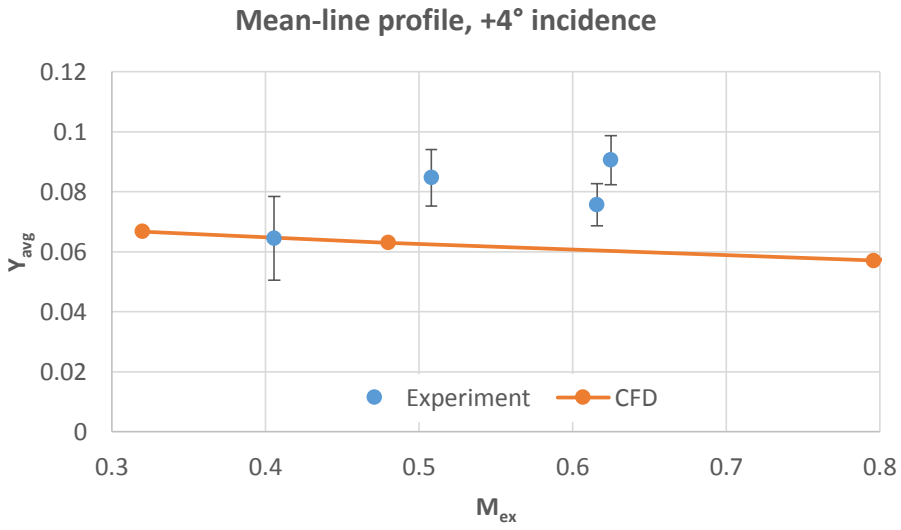

Figure 23. Area-averaged losses versus exit Mach number for mean-line profile, +4° incidence.

One may notice that the losses predicted by CFD do not vary significantly with incidence. In fact, this is the case. As Nunes [17] points out, the CFD simulations show virtually no difference in loss coefficient over the incidence range ±6°.

Placing the experimental data on the same plot, Figure 24 shows this is true for the experimental cases as well. It appears that the losses of this blade are relatively insensitive to incidence angle over the range -6° to +4°. For clarity, only one of the nearly identical CFD curves appears in the figure.

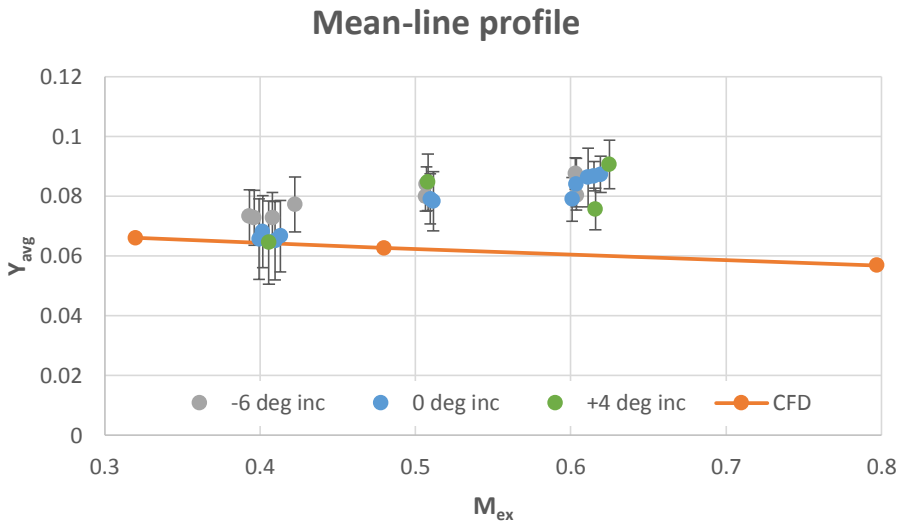

Figure 24. Area-averaged losses versus exit Mach number for the mean-line profile.

The geometric parameters and blade loading show that the mean-line profile is similar to the near-tip profile. This similarity holds for area-averaged loss coefficient as well, as shown by Figure 25. Here, even the sensitivity to exit Mach number seems to temper, with measured area-averaged losses of approximately 0.08 over the entire test range. Nunes [17] performed some limited study of the near-tip profile, which appears in the appendix of his work. It does not include a comprehensive study of losses similar to his results for the mean-line profile.

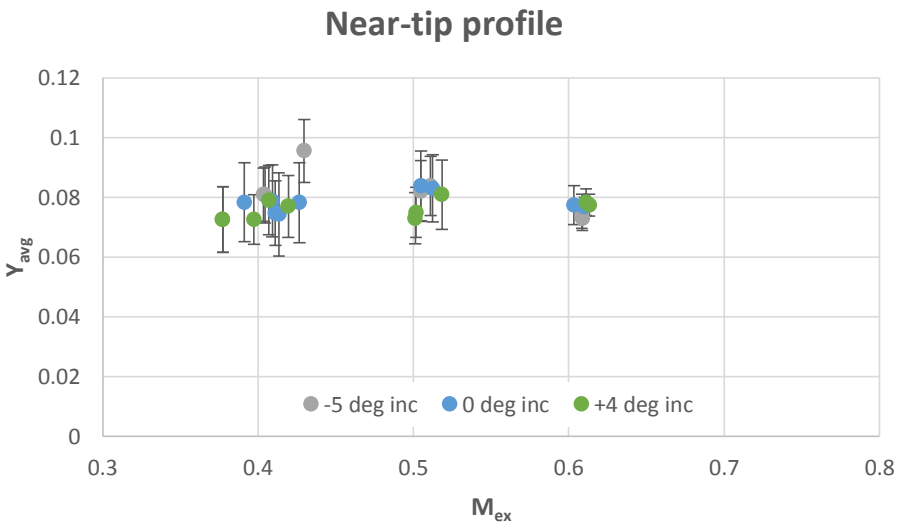

Figure 25. Area-averaged losses versus exit Mach number for the near-tip profile.

5. Conclusions

There is an apparent dearth of experimental results for modern low-reaction steam turbine blades in the open literature. As long as turbine designers continue to use profile loss models, however, there will be a need to continue correlating those tools with the experiments on the most recent designs. This study attempted to provide some of that needed data.

The loading of this blade had several unique features. Since it was low-reaction, the acceleration through the passage was much lower than that seen on the high-reaction blades in modern gas turbines. It also featured a "crossover" of the pressure and suction sides at the leading edge. A review of the current literature did not reveal any blades with similar loading.

The blade loading showed a close match with a CFD analysis on the same profile and was very similar between the mean-line and near-tip profiles. Changing the incidence angle to -6° increased the loading by 6%, while moving to +4° decreased loading by 3%. Only the leading edge saw the changes contributing to these values, loading was nearly identical on the aft 80% of the blades. Increasing the exit Mach number from 0.4 to 0.6 did not qualitatively alter the blade loading.

Despite extensive efforts to control flow at the top and bottom of the cascade and to reduce the effect of the serpentine exit flowpath, there was a noticeable aperiodicity in the local loss coefficients. In some cases, this accounted for over 10% uncertainty in the area-averaged losses. Future studies of this kind would do well to design a cascade to bring the flow to the leading edge of the top and bottom blades and employ an exhaust in line with the blade exit angle.

Contrary to the CFD results, area-averaged losses for the mean-line profile appeared to increase with increasing exit Mach number. Though much of the increase was within experimental uncertainty, the losses for exit Mach numbers of 0.5 and 0.6 were significantly higher than CFD results, up to 30% at the higher end of the range. The mechanism for this increase was an apparent deepening in the blade wakes in the experimental results that CFD did not predict.

Area-averaged losses for the near-tip profile did not significantly increase with increasing exit Mach number. Neither profile indicated changes in area-averaged losses with incidence angle. This is likely the intent of the blade designer. Since steam turbines often run at off-design conditions, having a blade insensitive to incidence angle changes over a ten-degree range would be desirable.

Overall, both profiles of the blade show very low losses over the range of exit Mach numbers and incidence angles tested. Fully characterizing the blade would require testing at greater off-design incidence angles to induce flow separation and at higher exit Mach numbers to

investigate transonic effects. The results presented in this study, however, are useful for the further refinement of empirical profile loss models.

References

[1] Ainley, D., and Mathieson, G., 1951, An examination of the flow and pressure losses in blade rows of axial-flow turbines, HM Stationery Office.
[2] Denton, J. D., 1993, "The 1993 Igti Scholar Lecture - Loss Mechanisms in Turbomachines," J Turbomach, 115(4), pp. 621-656.
[3] Blank, D. A. R. D. J. B. A. E., 1985, Introduction to naval engineering, Naval Institute Press, Annapolis, Md.
[4] Ainley, D., 1948, "Performance of axial-flow turbines," Proceedings of the Institution of Mechanical Engineers, 159(1), pp. 230-244.
[5] Hill, P. G., and Peterson, C. R., 1992, "Mechanics and thermodynamics of propulsion," Reading, MA, Addison-Wesley Publishing Co., 1992, 764 p., 1.
[6] Horlock, J. H., 1960, "Losses and efficiencies in axial-flow turbines," International Journal of Mechanical Sciences, 2(1-2), pp. 48-75.
[7] Craig, H., and Cox, H., 1970, "Performance estimation of axial flow turbines," Proceedings of the Institution of Mechanical Engineers, 185(1), pp. 407-424.
[8] Dunham, J., and Came, P. M., 1970, "Improvements to the Ainley-Mathieson Method of Turbine Performance Prediction," Journal of Engineering for Power, 92(3), p. 252.
[9] Kacker, S. C., and Okapuu, U., 1982, "A Mean Line Prediction Method for Axial-Flow Turbine Efficiency," J Eng Power-T Asme, 104(1), pp. 111-119.
[10] Havakechian, S., and Greim, R., 1999, "Aerodynamics design of 50 percent reaction steam turbines," P I Mech Eng C-J Mec, 213(1), pp. 1-25.
[11] Wei, N., 2000, "Significance of loss models in aerothermodynamic simulation for axial turbines," KTH.
[12] Bakhtar, F., Ebrahimi, M., and Bamkole, B., 1995, "On the Performance of a Cascade of Turbine Rotor Tip Section Blading in Nucleating Steam: Part 2: Wake Traverses," Proceedings of the Institution of Mechanical Engineers, Part C: Journal of Mechanical Engineering Science, 209(3), pp. 169-177.
[13] Li, S. M., Chu, T. L., Yoo, Y. S., and Ng, W. F., 2004, "Transonic and low supersonic flow losses of two steam turbine blades at large incidences," J Fluid Eng-T Asme, 126(6), pp. 966-975.
[14] Song, B., Ng, W. F., Cotroneo, J. A., Hofer, D. C., and Siden, G., 2007, "Aerodynamic design and testing of three low solidity steam turbine nozzle cascades," J Turbomach, 129(1), pp. 62-71.
[15] Bakhtar, F., Ebrahimi, M., and Webb, R., 1995, "On the Performance of a Cascade of Turbine Rotor Tip Section Blading in Nucleating Steam: Part 1: Surface Pressure Distributions," Proceedings of the Institution of Mechanical Engineers, Part C: Journal of Mechanical Engineering Science, 209(2), pp. 115-124.
[16] Abraham, S., Panchal, K., Xue, S., Ekkad, S. V., Ng, W., Brown, B. J., and Malandra, A., "Experimental and Numerical Investigations of a Transonic, High Turning Turbine Cascade With a Divergent Endwall," ASME.
[17] Nunes, B., 2013, "Numerical Loss Prediction of High Pressure Steam Turbine Rotor Airfoils."
[18] Kline, S. J., and McClintock, F., 1953, "Describing uncertainties in single-sample experiments," Mechanical engineering, 75(1), pp. 3-8.